

Optimization of Ship Stability through Response Surface Methodology: Enhancing Safety and Performance via Cross Curve Analysis

Kukuh Izatullah E.H.A.¹, Muhammad Arif Budiyanto², Wanda Rulita Sari³

(Received: 27 May 2024 / Revised: 10 June 2024 / Accepted: 13 June 2024)

Abstract—Optimizing the cross curves of ship stability through the application of Response Surface Methodology (RSM) requires a complex interplay between factors such as hull shape, beam, and draft significantly influences a ship's stability, which is crucial for the safety of the crew, passengers, and cargo. By employing RSM, this research systematically examines these factors, developing a second-order polynomial model to describe their relationship with stability metrics. The experiments were conducted using Design-Expert 13® software, which facilitated the design of experiments, data collection, model development, and validation. The optimized model revealed that while the overall impact of individual factors might not be significant, their combined interactions provide a robust predictive capability for ship stability. The results demonstrated that the optimized input variables led to improved stability outcomes, minimizing moment trim while maximizing longitudinal and transverse metacentric heights, thereby ensuring better performance and safety across various sea conditions.

Keywords— Ship Stability; Response Surface Methodology; Cross Curve Optimization; Metacentric Height; Design of Experiments

I. INTRODUCTION

Ships are complex forms of transportation that offer significant advantages [1], such as large capacity and efficiency in transporting goods and people around worldwide [2], [3]. However, their complexity also presents numerous challenges, particularly in ensuring safety because it's equipped with various essential systems for their safe operation, including navigation, communication, and propulsion systems [4]. These systems must be systematically designed, installed, and maintained to operate reliably and efficiently, which is crucial for the safety of the crew, passengers, and the environment. One critical system is the ballast system, which plays an important role in maintaining the ship's stability throughout its voyage [5], [6]. This system involves regulating the water in ballast tanks, which are designed to adjust the ship's balance and stability by adding or removing water as necessary [7]. This process is crucial for ensuring the safety of the ship, its crew, and the cargo it carries.

Stability can be represented as a cross curve [8], a graphical representation that illustrates the relationship between the righting lever and the angle of heel for a ship, which determines the ship's ability to recover from a list or heel caused by external forces like waves or wind. A higher righting lever indicates greater stability, allowing the ship to recover more effectively from a list, while a lower righting lever indicates less stability, making the ship more prone to capsizing [9]. Therefore, the cross

curve plays a vital role in assessing and ensuring the ship's ability to resist capsizing. Optimizing the cross curve is essential for ensuring the safety and efficiency of a ship [10], which involves designing the ship's hull and superstructure to maximize the righting lever across a range of heel angles, with the goal of achieving a high maximum righting lever and a wide stability range. This optimization allows the ship to operate safely in various sea conditions. Research on optimizing cross curves is conducted by Lian *et al.* [11], with focusing on the impact of various design parameters such as hull shape, beam, and draft on the ship's stability for improved safety.

One of the most widely used and effective optimization techniques in various fields is response surface methodology (RSM), as well as implementing it into ship stability analysis. The use of RSM for optimizing the cross curve in ship stability analysis has been demonstrated in various studies. Sun *et al.* [12] used RSM to optimize process parameters in the casting, welding, and machinability studies of composite materials, highlighting the potential of RSM for improving ship stability. RSM is particularly useful when multiple factors interact and influence the outcome of a process to optimize the cross curve by identifying the most critical factors affecting the ship's stability. These factors include design parameters and operational factors to decide the cross curve optimization which made RSM being a powerful optimization technique that can be effectively applied to optimize the cross curve in ship stability analysis for its ability to handle complex interactions between factors.

Kukuh Izatullah E.H.A., Departement of Mechanical Engineering, Universitas Indonesia, Depok, 16424, Indonesia. E-mail: kukuh.izatullah@ui.ac.id

Muhammad Arif Budiyanto, Departement of Mechanical Engineering, Universitas Indonesia, Depok, 16424, Indonesia. E-mail: arif@eng.ui.ac.id

Wanda Rulita Sari, Departement of Mechanical Engineering, Universitas Indonesia, Depok, 16424, Indonesia. E-mail: wanda.rulita@ui.ac.id

A. Ship Stability

As explained in the previous section that the ballast system is directly linked to the stability of the ship, as it helps to achieve and maintain the desired balance of the vessel. This balance is critical for several reasons: ballast water is used to adjust the ship's trim, which is the angle at which the ship sits in the water with the proper trim [12]. Ensuring the safety of a ship, its crew, and its cargo relies heavily on ship stability, which encompasses both static and dynamic aspects [13]. Static stability pertains to the ship's resistance to capsizing while at rest or moving steadily, relying on factors like the center of gravity (CG), center of buoyancy (CB), and metacentric height (GM) [14], where a higher GM signifies enhanced stability. Conversely, dynamic stability addresses the ship's ability to withstand capsizing when subjected to external forces like waves and wind, involving parameters such as the righting lever (GZ) and the angle of heel [15]. A pivotal tool in analyzing ship stability is the cross curve, which delineates the maximum righting lever (GZMAX) at the point of inflection, where the ship's stability is at its zenith. By deciphering this curve, designers and operators can ascertain optimal loading conditions, ensuring the ship's safety and efficacy across diverse sea conditions.

B. Response Surface Methodology

Response Surface Methodology (RSM) is extensively employed for optimization in diverse fields, including the complex analysis of ship stability and ship structures [16], [17]. It proves particularly valuable when multiple interacting factors complicate to utilized for refine the cross curve, identifying critical factors influencing a vessel's stability. The RSM process involves several essential stages: The design of experiments constructs a set of trials to manipulate specific factors while holding others constant [18]. Model development entails creating a mathematical representation of the relationship between factors and the response variable, typically as a second-order polynomial equation [19], [20]. Model validation ensures the accuracy of the model's predictions by comparing them with empirical data, confirming its ability to capture the inherent relationships between factors and responses [21]. The optimization phase is the process of validated model that guides the search for the optimal combination of factors to achieve the desired outcome,

typically involving maximizing or minimizing the response variable.

II. METHODOLOGY

A. Research Design

The research design start with the preparation of ship data used for cross curve stability analysis, Anchor Handling Tugs ship type obtained from Figure 1, and the ship particulars in Table 1. The input and output factors used in this analysis are listed in Table 4 that has been validated by Maxsurf®, with input factors and output factors as the measured responses. The experiments used Design-Expert 13® to vary the identified input factors, using the Design of Experiments (DOE) approach to Central Composite Design, to determine the combinations of input factors to be evaluated [22]. The experimental data is entered into Design-Expert 13® to develop a mathematical model, typically a second-order polynomial equation that describes the relationship between the input factors and the output. The developed model is then validated by comparing the model's predictions with the actual experimental results, ensuring the model's accuracy in capturing the relationship between the input factors and the output. Once validated, the model is used for optimization to find the optimal combination of input factors that result in the best cross curve stability and identify the optimal points by maximizing or minimizing the response variable.

B. Research Variables

In the CCD method, there are two types of factors: input and output factors [23]. Input factors are the variables manipulated or controlled during the process. These factors can be continuous or categorical and are typically represented by a set of levels or inputs [24], like in Table 3. Output factors, also known as response variables, are the variables measured or observed as a result of the process [25]. These variables are typically continuous and used to evaluate the process's performance. Like input factors, output factors are represented by a set of levels or values. The input and output variables on this reasearch are described on the Table 2.

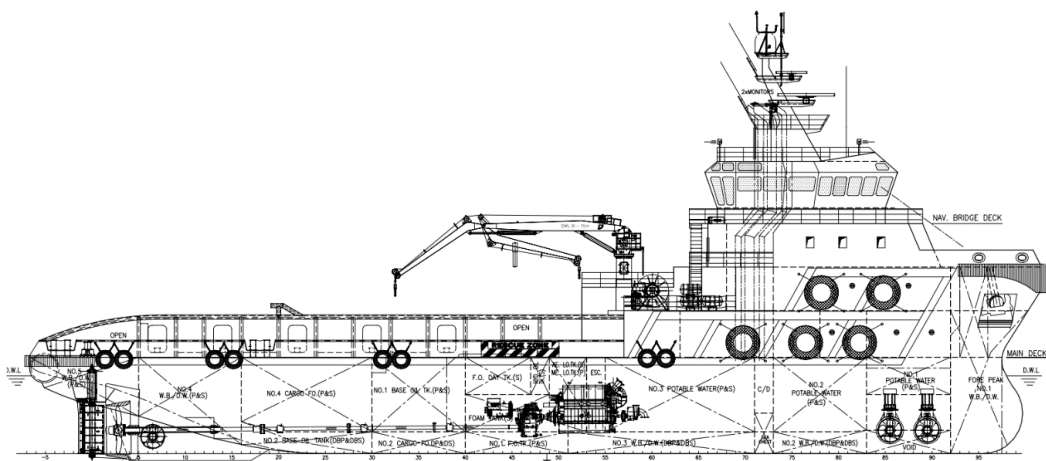


Figure 1. Outboard Profile of Anchor Handling Tug Vessels

TABLE 1.
SHIP PRINCIPLE PARTICULAR

Ship Particular	Value	Unit
LOA	65	m
LBP	58.5	m
Beam Moulded	16	m
Depth Moulded	6.2	m
Draft Designed	5	m
Draft Maximum	5	m
Displacement	3821.96	ton
Deadweight	1981.052	ton

TABLE 2.
TYPE FACTOR OF VARIABLE

Type Factor	Factor	Explanation
Input	Draft LCF (Longitudinal Center of Flotation)	Indicates the ship's draft at the point where its center of gravity meets the waterline and is used to determine important stability metrics such as the righting lever and the metacentric height [26].
	Disp (Displacement)	Indicating the volume of water a ship displaces is calculated by multiplying the ship's volume by the density of the water to determine the ship's buoyancy and overall stability [27].
	LCB (Longitudinal Center of Buoyancy)	The center of buoyancy relative to a specific reference point on the ship, typically measured from the forward perpendicular (FP) or amidships and expressed as a ratio of the waterline length (LWL) that affecting the vessel's longitudinal stability [28], [29].
	VCB (Vertical Center of Buoyancy)	The height of the buoyancy center relative to the ship's reference points was measured from the base line and expressed as a ratio of the waterline length (LWL), which had an impact on vertical stability [30], [31].
	Weight	Representing the total downward force exerted on the ship, which includes the combined weights of the total ship weight, with an additional margin for underestimated weights, and estimating the weights to ensure the ship does not exceed its design capacity due to the affected stability [32].
Output	LCF (Longitudinal Center of Flotation)	The spot where the ship's waterline intersects its centerline acts as the pivot point for longitudinal weight shifts that cause the ship to trim and is measured from either the after perpendicular (AP) or the midships perpendicular (MP), dictating the ship's reaction to alterations in weight distribution [33].
	Moment Trim	Indicating the force needed to modify the vessel's trim and representing the moment required to adjust the ship's trim by precisely one centimeter, which is determined by multiplying the ship's weight by the distance from the center of flotation (COF), where longitudinal weight adjustments occur, and performance across diverse loading conditions [34], [35].
	KML (Metacentric Height Longitudinal)	Indicating the distance between a ship's longitudinal center of buoyancy (LCB) and its longitudinal center of flotation (LCF) holds utmost significance in ship stability analysis because it impacts the vessel's longitudinal stability and its resilience against capsizing [36].
	KMT (Metacentric Height Transverse)	Signifying the distance between a ship's center of buoyancy and its center of flotation in the transverse direction and impacting the vessel's transverse stability and its resilience against capsizing [37].

TABLE 3.
 INPUT FACTOR VALUE

Input Factor	Factor Value
Draft LCF	$0.5 \leq A \leq 0.78$
Disp	$287.74 \leq B \leq 463.390$
LCB	$29.745 \leq C \leq 29.874$
VCB	$0.245 \leq D \leq 0.395$
Weight	$6.08 \leq E \leq 6.38$
LCF	$29.839 \leq F \leq 30.141$

TABLE 4.
 INPUT AND OUTPUT PARAMETER

Input						Output		
Draft LCF [m]	Disp [Metric Ton]	LCB [m]	VCB [m]	Weight [Ton]	LCF [m]	Moment Trim [Metric Ton Meter]	KML [m]	KMT [m]
0.500	287.740	29.745	0.245	6.080	30.141	15.850	322.240	33.638
0.510	293.830	29.753	0.250	6.100	30.140	15.920	317.030	33.116
0.520	299.940	29.761	0.256	6.110	30.137	16.000	312.040	32.615
0.530	306.070	29.769	0.261	6.130	30.134	16.080	307.270	32.132
0.540	312.210	29.776	0.266	6.150	30.131	16.150	302.590	31.663
0.550	318.360	29.782	0.272	6.160	30.128	16.220	298.090	31.206
0.560	324.530	29.789	0.277	6.180	30.124	16.300	293.780	30.765
0.570	330.710	29.795	0.283	6.190	30.130	16.350	289.230	30.334
0.580	336.910	29.801	0.288	6.200	30.128	16.420	285.120	29.921
0.590	343.120	29.807	0.293	6.220	30.126	16.490	281.130	29.520
0.600	349.340	29.813	0.299	6.230	30.123	16.560	277.270	29.129
0.610	355.580	29.818	0.304	6.240	30.122	16.620	273.490	28.748
0.620	361.830	29.824	0.309	6.260	30.121	16.690	269.850	28.381
0.630	368.090	29.829	0.315	6.270	30.118	16.760	266.350	28.025
0.640	374.370	29.833	0.320	6.280	30.116	16.830	262.950	27.676
0.650	380.660	29.838	0.326	6.300	30.114	16.890	259.620	27.336
0.660	386.970	29.842	0.331	6.310	30.111	16.960	256.400	27.007
0.670	393.290	29.846	0.336	6.320	30.109	17.030	253.300	26.688
0.680	399.620	29.850	0.342	6.340	30.106	17.100	250.290	26.377
0.690	405.960	29.854	0.347	6.350	30.101	17.170	247.390	26.072
0.700	412.320	29.858	0.352	6.360	30.099	17.230	244.490	25.775
0.710	418.690	29.862	0.358	6.370	30.097	17.300	241.680	25.485
0.720	425.060	29.865	0.363	6.390	30.095	17.360	238.960	25.203
0.730	431.460	29.869	0.368	6.400	30.092	17.430	236.310	24.929
0.740	437.850	29.872	0.374	6.390	30.025	17.340	231.620	24.628
0.750	444.240	29.873	0.379	6.380	29.956	17.230	226.890	24.365
0.760	450.620	29.874	0.385	6.380	29.915	17.200	223.240	24.100
0.770	457.010	29.875	0.390	6.380	29.874	17.160	219.680	23.843
0.780	463.390	29.874	0.395	6.380	29.839	17.140	216.420	23.594

C. Analysis

The analysis of a design of experiment using central composite design (CCD) involves several key steps that begin with establishing the experimental design, where

CCD, a type of recommended models and optimizes complex processes by selecting independent variables, their levels, and conducting the experiments [38]. Following this, the data collected from these experiments

is used to develop a mathematical model, typically a second-order polynomial equation, to describe the relationship between the independent and response variables [39]. This model undergoes analysis using analysis of variance (ANOVA) to determine the significance of its terms. The results from ANOVA are then used to create equation formulas that detail the relationships between the independent and response variables. After that, the analysis results are presented in graphic plots, such as normal residuals, residual vs. predicted, and 3D surface plots, which help visualize these relationships and identify patterns or trends in the data.

III. RESULTS AND DISCUSSION

In an RSM analysis using the input and output parameters from Table 4, data from 30 samples were evaluated for ship stability cross curves. The analysis employed a fractional mathematical model for the

response factor of Moment Trim on Equation (1). The 2FI model results for ANOVA on Moment Trim shown on the Table 5 has a sum of squares of 6.81 with 21 degrees of freedom (df), yielding a mean square of 0.3242 and an F-value of 11193.7, which is significant with a p-value < 0.0001. However, the individual analysis of parameters such as Draft LCF, Displacement (Disp), Longitudinal Center of Buoyancy (LCB), Vertical Center of Buoyancy (VCB), Weight, and Longitudinal Center of Flotation (LCF) revealed that each parameter had a p-value significantly above 0.05, indicating that none of these parameters were individually significant to the response Moment Trim. The residual value is 0.0002 with 8 degrees of freedom, while the Cor Total remains 6.81 with 29 degrees of freedom. These results indicate that while the overall model is significant, the individual contributions of the parameters to the moment trim are not significant as can be seen on the Figure 1.

TABLE 5.
 2FI MODEL RESULT FOR ANOVA ON MOMENT TRIM

Source	Sum of Squares	df	Mean Square	F-value	p-value	
Model	6.81	21	0.3242	11193.7	< 0.0001	significant
A-Draft LCF	3.47E-07	1	3.47E-07	0.012	0.9155	
B-Disp	4.09E-07	1	4.09E-07	0.0141	0.9084	
C-LCB	5.65E-06	1	5.65E-06	0.1952	0.6704	
D-VCB	2.99E-07	1	2.99E-07	0.0103	0.9215	
E-Weight	1.34E-06	1	1.34E-06	0.0463	0.835	
F-LCF	0	1	0	0.3961	0.5466	
Residual	0.0002	8	0			
Cor Total	6.81	29				

$$\begin{aligned}
 \text{Moment Trim} = & +16.96 - 6.44A + 6.94B - 0.2248C + 0.3042D - 0.0999E - 0.1494F + 4.58AB - 11.49AC \\
 & - 119.62AD + 105.62AE - 17.55AF + 10.06BC + 111.25BD - 104.37BE + 18.76BF \\
 & + 5.31CD - 3.21CE + 1.38CF + 2.03DE - 1.94DF - 0.0039EF
 \end{aligned}
 \tag{1}$$

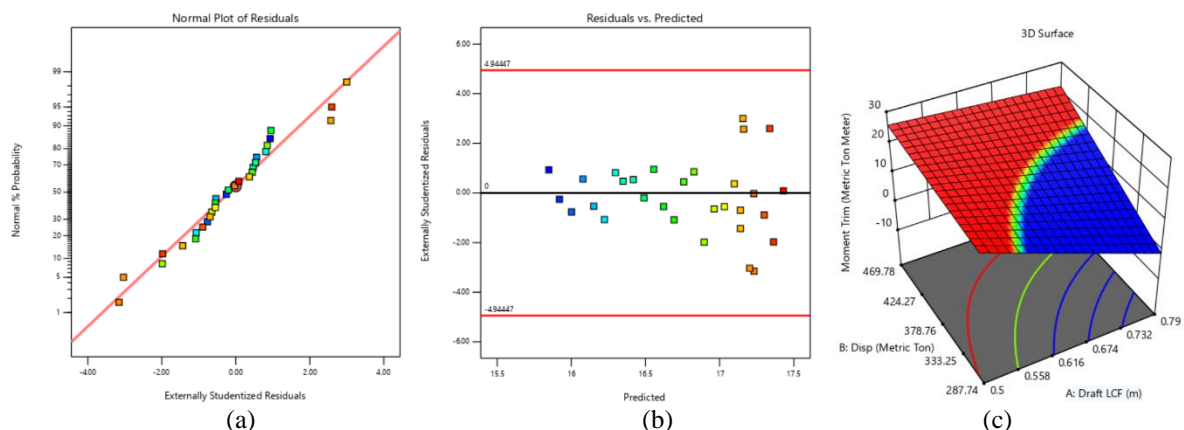


Figure 2. Moment Trim Variables Graphs a) Normal Plot of Residuals b) Residual vs Predicted c) 3D Surface Relations

The ANOVA for KML demonstrated a p-value of <0.0001, underscoring the model's significance that can be seen on Table 6. Similar to Moment Trim, individual factors like Draft LCF, Disp, LCB, VCB, Weight, and LCF had non-significant p-values individually, yet their combined interactions provided a robust model. With a predicted R² of 0.9998 and an adjusted R² of 1.0000, the model shows outstanding accuracy with the mathematical representation in Equation (2) along with the interrelationships between response factors in Figure 2.

The ANOVA for KMT revealed a Sum of Squares of 276.7, a Mean Square of 13.18, an F-value of 5.48E+06, and a p-value of <0.0001, confirming the model's high significance. Although individual p-values for factors such as Draft LCF, Disp, LCB, VCB, Weight, and LCF were not significant on their own, the overall model was highly predictive. The predicted and adjusted R² values both being 1.0000 indicate perfect model fit, predictive accuracy that presented by mathematical model in Equation (3), and the results diagram in Figure 3.

TABLE 6.
 2FI MODEL RESULT FOR ANOVA ON KMT

Source	Sum of Squares	df	Mean Square	F-value	p-value	significant
Model	29406.58	21	1400.31	4.94E+05	< 0.0001	significant
A-Draft LCF	0	1	0	0.0099	0.9232	
B-Disp	0.0001	1	0.0001	0.0336	0.8592	
C-LCB	0.0017	1	0.0017	0.6169	0.4548	
D-VCB	0.0001	1	0.0001	0.0233	0.8825	
E-Weight	0.0004	1	0.0004	0.1284	0.7293	
F-LCF	0.0072	1	0.0072	2.53	0.1505	
Residual	0.0227	8	0.0028			
Cor Total	29406.61	29				

$$\begin{aligned}
 KMT = & +260.94 + 57.87A - 106.02B - 3.95C - 4.52D - 1.65E - 3.73F + 79.30AB - 158.02AC - 1167.92AD \\
 & + 1119.73AE - 120.83AF + 143.74BC + 1053.65BD - 1118.25BE + 134.97BF + 63.33CD \\
 & - 35.91CE + 17.15CF + 36.26DE - 23.69DF + 1.54EF
 \end{aligned}
 \tag{2}$$

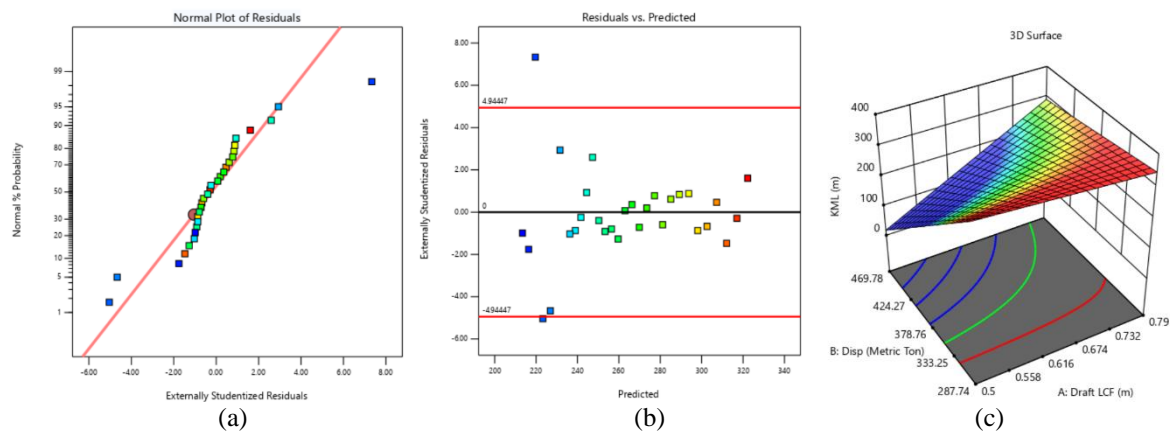


Figure 3 KMT Variables Graphs a) Normal Plot of Residuals; b) Residual vs Predicted; c) 3D Surface Relations

TABLE 7.
 2FI MODEL RESULT FOR ANOVA ON KML

Source	Sum of Squares	df	Mean Square	F-value	p-value	significant
Model	276.7	21	13.18	5.48E+06	< 0.0001	significant
A-Draft LCF	2.35E-06	1	2.35E-06	0.979	0.3514	
B-Disp	1.17E-06	1	1.17E-06	0.4884	0.5044	
C-LCB	1.79E-06	1	1.79E-06	0.7439	0.4135	
D-VCB	3.31E-07	1	3.31E-07	0.1378	0.7201	
E-Weight	4.13E-06	1	4.13E-06	1.72	0.2264	
F-LCF	7.33E-06	1	7.33E-06	3.05	0.1189	
Residual	0	8	2.40E-06			
Cor Total	276.7	29				

$$\begin{aligned}
 KMT = & +27.87 - 16.77A + 11.78B - 0.1264C - 0.3201D + 0.1753E - 0.1194F - 7.65AB + 17.60AC \\
 & - 98.64AD + 77.78AE - 57.77AF - 18.31BC + 101.52BD - 66.15BE + 53.55BF + 5.44CD \\
 & - 3.83CE + 1.36CF - 7.29DE + 2.16DF + 0.5494EF
 \end{aligned}
 \tag{3}$$

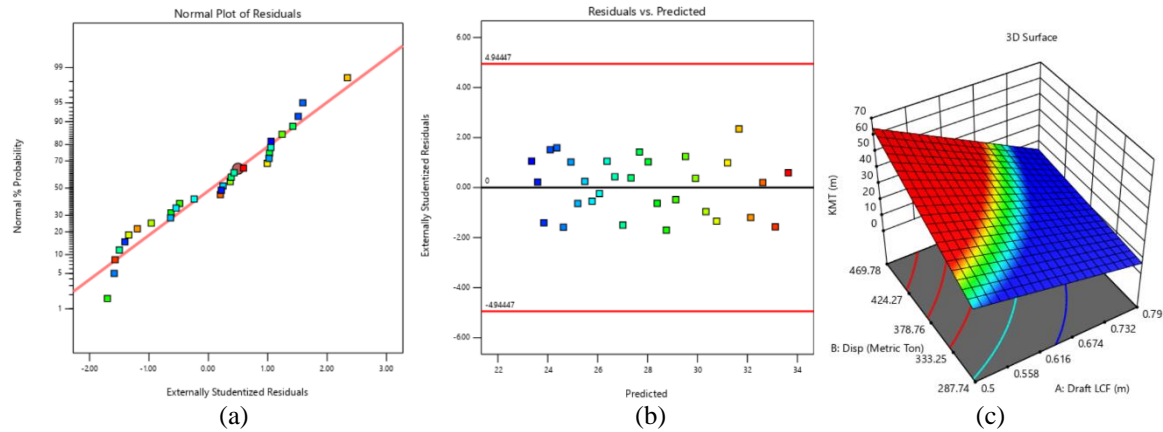


Figure 4. KML Variables Graphs a) Normal Plot of Residuals; b) Residual vs Predicted; c) 3D Surface Relations

The optimization process involved setting criteria for six input and three output variables, as illustrated in Figure 5. All input variables were maintained within their specified range values to ensure feasible and practical solutions. For the output variables, the criteria were set to minimize the moment trim, maximize the longitudinal metacentric height (KML), and maximize the transverse

metacentric height (KMT). This approach aimed to optimize the ship's stability by achieving the most favorable combination of input variables that would result in the desired performance outcomes for the response variables. The optimization ensured that the ship would have the best possible stability characteristics under various loading and operational conditions.

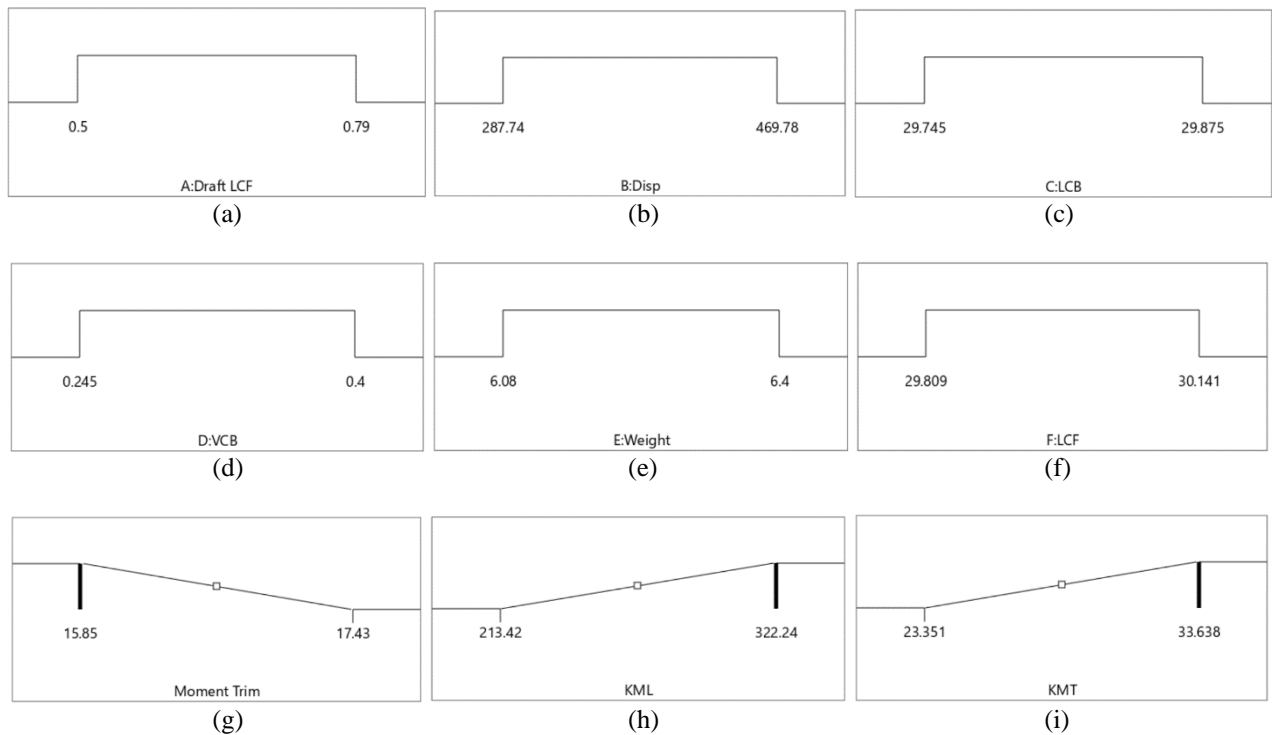


Figure 5 Optimization Value Set Process a) Draft LCF; b) Disp; c) LCB; d) VCB; e) Weight; f) LCF; g) Moment Trim; h) KML; i) KMT

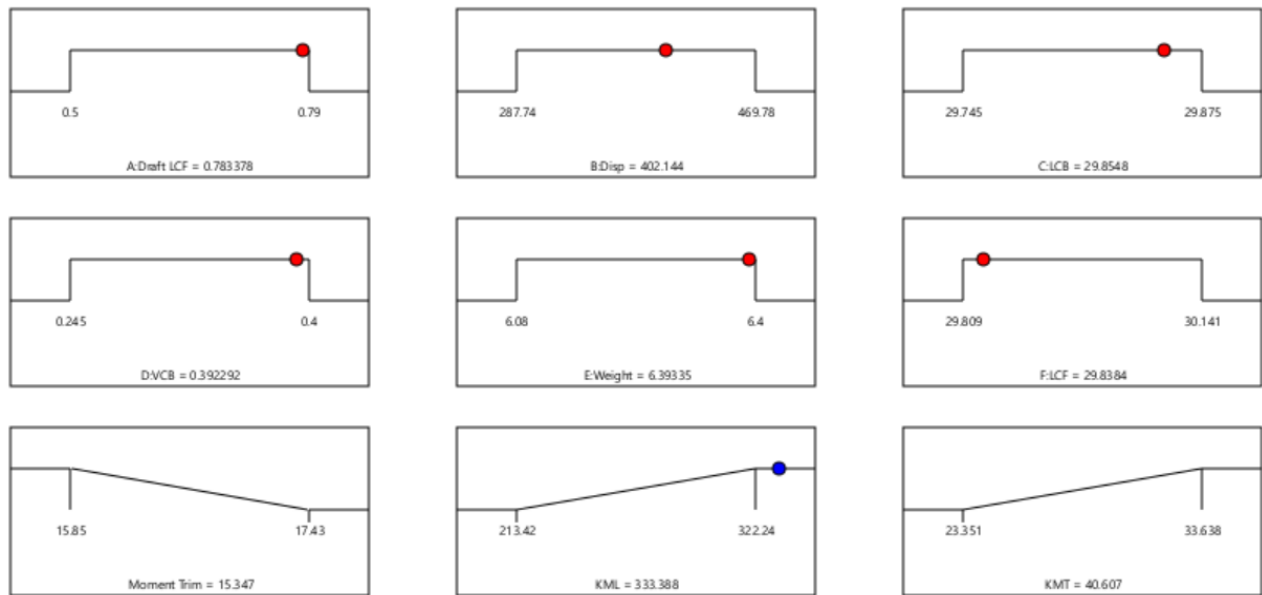


Figure 6. Optimization Result Value

Based on the optimization criteria previously set, the resulting values for each variable were determined as follows. For the input variables, the draft at the Longitudinal Center of Flotation (Draft LCF) was 0.783378 meters, the displacement (Disp) was 402.144 tons, the Longitudinal Center of Buoyancy (LCB) was positioned at 29.8548 meters, the Vertical Center of Buoyancy (VCB) was at 0.392292 meters, and the total weight was 6.39335 tons. These input values were carefully selected to achieve the optimal stability conditions. For the output or response variables, the moment trim was minimized to 15.347, while the longitudinal metacentric height (KML) was maximized to 333.388 meters, and the transverse metacentric height (KMT) was maximized to 40.607 meters. These results indicate that the optimization process successfully balanced the inputs to enhance the ship's stability, achieving the desired performance in minimizing moment trim and maximizing both KML and KMT.

IV. CONCLUSION

The empirical results of this study demonstrate the significant impact of using Response Surface Methodology (RSM) to optimize ship stability parameters. Analyzing 30 samples with varying inputs, the study constructed a robust model that minimized moment trim to 15.347 and maximized both longitudinal metacentric height (KML) to 333.388 meters and transverse metacentric height (KMT) to 40.607 meters, ensuring improved balance and stability. ANOVA results showed that individual factors such as Draft LCF, Displacement, Longitudinal Center of Buoyancy, Vertical Center of Buoyancy, Weight, and Longitudinal Center of Flotation were not significant on their own but formed a highly predictive model when combined. The predicted and adjusted R^2 values of 1.0000 for KML and KMT reflect the model's excellent accuracy. The application of RSM in this study effectively enhanced ship stability, underscoring the importance of considering multiple

interacting factors for more reliable ship design and operation.

ACKNOWLEDGEMENTS

The author expresses profound gratitude to Prof. Dr.-Ing. Nasruddin, the esteemed lecturer of Design of Experiment in the Magister of Mechanical Engineering at Universitas Indonesia, for his invaluable guidance and support throughout this research. His expertise and encouragement have been instrumental in the successful completion of this study.

REFERENCES

- [1] L. Wang, H. Yu, X. Wei, and H. B. T.-R. M. in C. Liu Molecular Sciences and Chemical Engineering, "Applications – Transportation | Ships: Fuel cells, batteries," Elsevier, 2023. doi: <https://doi.org/10.1016/B978-0-323-96022-9.00135-3>.
- [2] L. Meng, X. Wang, J. He, and C. Han, "Ship allocation considering energy type and transportation preference: A variational inequality approach," *Adv. Eng. Informatics*, vol. 59, no. September 2023, p. 102291, 2024, doi: 10.1016/j.aei.2023.102291.
- [3] A. Godet, J. N. Nurup, J. T. Saber, G. Panagakos, and M. B. Barfod, "Operational cycles for maritime transportation: A benchmarking tool for ship energy efficiency," *Transp. Res. Part D Transp. Environ.*, vol. 121, no. June, p. 103840, 2023, doi: 10.1016/j.trd.2023.103840.
- [4] M. Xu, X. Ma, Y. Zhao, and W. Qiao, "A Systematic Literature Review of Maritime Transportation Safety Management," *J. Mar. Sci. Eng.*, vol. 11, no. 12, 2023, doi: 10.3390/jmse11122311.
- [5] A. Morska, P. Krata, W. Wawrzyński, W. Więckiewicz, and J. Jachowski, "Ship's ballast tanks size and dimensions review for the purpose of model research into the liquid sloshing phenomenon," *Sci. Journals Marit. Univ. Szczecin*, vol. 29, no. 101, pp. 88–94, 2012.
- [6] A. Malakhov, A. Palagin, I. Maslov, and R. Gudilko, "Improvement of ship ballasting system," *Technol. Audit Prod. Reserv.*, vol. 4, no. 1(36), pp. 25–29, 2017, doi: 10.15587/2312-8372.2017.109087.
- [7] A. Kurniawan, Hardianto, E. S. Koenhardono, and I. R. Kusuma, "Modeling and control of ballast system to improve stability of catamaran boat," *ICAMIMIA 2015 - Int. Conf. Adv. Mechatronics, Intell. Manuf. Ind. Autom. Proceeding - conjunction with Ind. Mechatronics Autom. Exhib. IMAE*, vol. 2015, no. Icamimia, pp. 202–204, 2016, doi: 10.1109/ICAMIMIA.2015.7508032.
- [8] Y. Hu, J. Tang, S. Xue, and S. Liu, "Stability criterion and its

- calculation for sail-assisted ship,” *Int. J. Nav. Archit. Ocean Eng.*, vol. 7, no. 1, pp. 1–9, 2015, doi: 10.2478/IJNAOE-2015-0001.
- [9] J. Womack and B. Johnson, “A Guide to Fishing Vessel Stability,” *Soc. Nav. Archit. Mar. Eng.*, 2017.
- [10] M. Vidić and I. Bačkalov, “An analysis of stability requirements for large inland passenger ships,” *Ocean Eng.*, vol. 261, no. March, 2022, doi: 10.1016/j.oceaneng.2022.112148.
- [11] J. Lian *et al.*, “Effects of damping plate on the motion response of transport ships under waves,” *Appl. Ocean Res.*, vol. 134, no. January, p. 103507, 2023, doi: 10.1016/j.apor.2023.103507.
- [12] E. Shivachev, M. Khorasanchi, S. Day, and O. Turan, “Impact of trim on added resistance of KRISO container ship (KCS) in head waves: An experimental and numerical study,” *Ocean Eng.*, vol. 211, no. April, p. 107594, 2020, doi: 10.1016/j.oceaneng.2020.107594.
- [13] K. Lapa, “Assessment of the stability of passenger ships in coastal navigation in case of lacking ship geometry data,” *Trans. Marit. Sci.*, vol. 9, no. 2, pp. 150–160, 2020, doi: 10.7225/toms.v09.n02.002.
- [14] V. Wilczynski and W. J. Diehlt, “An Alternative approach to determine a vessel’s center of gravity: the center of buoyancy method,” *Ocean Eng.*, vol. 22, no. 6, pp. 563–570, 1995.
- [15] Y. Jiang, M. Wang, J. Bai, Y. Sun, and J. Li, “Effects of outrigger configuration on trimaran stability in longitudinal waves,” *Ocean Eng.*, vol. 280, no. March, p. 114500, 2023, doi: 10.1016/j.oceaneng.2023.114500.
- [16] J. C. Lee, S. C. Shin, and S. Y. Kim, “An optimal design of wind turbine and ship structure based on neuro-response surface method,” *Int. J. Nav. Archit. Ocean Eng.*, vol. 7, no. 4, pp. 750–769, 2015, doi: 10.1515/ijnaoe-2015-0053.
- [17] M. Arai and T. Shimizu, “Optimization of the Design of Ship Structures Using Response Surface Methodology,” Y.-S. Wu, W.-C. Cui, and G.-J. B. T.-P. D. of S. and O. F. S. Zhou, Eds., Oxford: Elsevier Science Ltd, 2001, pp. 331–339. doi: <https://doi.org/10.1016/B978-008043950-1/50042-9>.
- [18] X. Chen, T. Takami, M. Oka, Y. Kawamura, and T. Okada, “Stochastic wave spectra estimation (SWSE) based on response surface methodology considering uncertainty in transfer functions of a ship,” *Mar. Struct.*, vol. 90, no. February, p. 103423, 2023, doi: 10.1016/j.marstruc.2023.103423.
- [19] A. Soleimani, M. Akbari, A. Karimipour, A. H. Meghdadi Isfahani, and R. Nosouhi, “Investigation the effect of dissimilar laser welding parameters on temperature field, mechanical properties and fusion zone microstructure of inconel 600 and duplex 2205 stainless steel via response surface methodology,” *Heliyon*, vol. 10, no. 4, p. e26010, 2024, doi: 10.1016/j.heliyon.2024.e26010.
- [20] A. K. Sahu, N. K. Sahu, A. K. Sahu, M. S. Rajput, and H. K. Narang, “Modeling the predictive values of ultimate tensile strength in welded joint by response surface methodology,” *Mater. Today Proc.*, vol. 44, pp. 3110–3114, 2021, doi: 10.1016/j.matpr.2021.02.798.
- [21] H. Öktem, T. Erzurumlu, and H. Kurtaran, “Application of response surface methodology in the optimization of cutting conditions for surface roughness,” *J. Mater. Process. Technol.*, vol. 170, no. 1–2, pp. 11–16, 2005, doi: 10.1016/j.jmatprotec.2005.04.096.
- [22] R. Madesh and G. K. K., “Multi-layer additive manufacturing on nickel-based superalloy by optimization of pulsed mode process parameters of single-layer bead geometry,” *Mater. Today Commun.*, vol. 37, no. July, p. 107463, 2023, doi: 10.1016/j.mtcomm.2023.107463.
- [23] S. J. S. Chelladurai, K. Murugan, A. P. Ray, M. Upadhyaya, V. Narasimharaj, and S. Gnanasekaran, “Optimization of process parameters using response surface methodology: A review,” *Mater. Today Proc.*, vol. 37, no. Part 2, pp. 1301–1304, 2020, doi: 10.1016/j.matpr.2020.06.466.
- [24] J. Wu, P. P. Gao, and X. Gao, “Optimization of Response Surface Methodology for Pulsed Laser Welding of 316L Stainless Steel to Polylactic Acid,” *Metals (Basel)*, vol. 13, no. 2, pp. 1–16, 2023, doi: 10.3390/met13020214.
- [25] N. A. Imhansoloeva, J. I. Achebo, K. Obahiagbon, J. O. Osarenmwinda, and C. E. Etin-Osa, “Optimization of the Deposition Rate of Tungsten Inert Gas Mild Steel Using Response Surface Methodology,” *Engineering*, vol. 10, no. 11, pp. 784–804, 2018, doi: 10.4236/eng.2018.1011055.
- [26] K. N. Lapa, “Estimation of stability for a fishing vessel and some considerations,” *IOP Conf. Ser. Mater. Sci. Eng.*, vol. 400, no. 8, 2018, doi: 10.1088/1757-899X/400/8/082014.
- [27] B. Barrass and D. R. Derret, *Ship Stability for Masters and Mates 6th Edition*, 6th ed. Elsevier, 2017.
- [28] D. Yang, X. Guo, L. Jiang, and T. Du, “Prediction model of buoyancy-driven flow rate in inclined tunnels with a localized buoyancy source: Emphasis on stratification effects,” *Build. Environ.*, vol. 250, no. January, p. 111165, 2024, doi: 10.1016/j.buildenv.2024.111165.
- [29] X. Sun, Y. Ni, C. Liu, Z. Wang, and Y. Yin, “A practical method for stability assessment of a damaged ship,” *Ocean Eng.*, vol. 222, no. September 2020, p. 108594, 2021, doi: 10.1016/j.oceaneng.2021.108594.
- [30] P. Furness, *Advanced Naval Architecture & Ship Construction*. Australian Maritime College, 2013.
- [31] A. Biran and R. López-Pulido, “Ship Hydrostatics and Stability: Second Edition,” *Sh. Hydrostatics Stab. Second Ed.*, pp. 1–392, 2013, doi: 10.1016/C2011-0-07795-5.
- [32] A. Mentés and H. Akyildiz, “Criticality analysis of probabilistic damage stability of ships with aggregation operators and additive ratio assessment,” *Ocean Eng.*, vol. 270, no. September 2022, p. 113577, 2023, doi: 10.1016/j.oceaneng.2022.113577.
- [33] F. Pérez-Arribas and J. Calderon-Sanchez, “A parametric methodology for the preliminary design of SWATH hulls,” *Ocean Eng.*, vol. 197, no. May 2019, 2020, doi: 10.1016/j.oceaneng.2019.106823.
- [34] M. Ok and H. Lei, “Accurate and robust linear representation for containership stability conditions with ballast water,” *Ocean Eng.*, vol. 306, no. May, p. 118141, 2024, doi: 10.1016/j.oceaneng.2024.118141.
- [35] C. G. Grlić, N. Degiuli, Ž. Tuković, A. Farkas, and I. Martić, “The effect of loading conditions and ship speed on the wind and air resistance of a containership,” *Ocean Eng.*, vol. 273, no. February, 2023, doi: 10.1016/j.oceaneng.2023.113991.
- [36] W. hua Wang, L. lin Wang, Y. zhen Du, and Y. Huang, “Novel controller for the coupled surge-pitch problem by controlling the metacentric height of sandglass-type FDPSO,” *Ocean Eng.*, vol. 251, no. March, p. 111095, 2022, doi: 10.1016/j.oceaneng.2022.111095.
- [37] S. Masamoto, N. Umeda, S. Subramaniam, and A. Matsuda, “Experimental study of the water on deck effects on the transverse stability of a fishing vessel running in stern quartering seas,” *Ocean Eng.*, vol. 289, no. P2, p. 116289, 2023, doi: 10.1016/j.oceaneng.2023.116289.
- [38] S. Z. Amraini *et al.*, “The use of fractional factorial design to analyze the effect of sulfuric acid concentration and temperature on furfural yield,” *Mater. Today Proc.*, vol. 87, pp. 240–245, 2023, doi: 10.1016/j.matpr.2023.03.101.
- [39] E. Ostertagová, “Modelling using polynomial regression,” *Procedia Eng.*, vol. 48, no. December 2012, pp. 500–506, 2012, doi: 10.1016/j.proeng.2012.09.545.